
5-1-2022

Mice Lacking Full Length Adgrb1 (bai1) Exhibit Social Deficits, Increased Seizure Susceptibility, and Altered Brain Development

Fu Hung Shiu
Emory University School of Medicine

Jennifer C. Wong
Emory University School of Medicine

Takahiro Yamamoto
University of Alabama at Birmingham School of Medicine

Trisha Lala
Emory University

Ryan H. Purcell
Emory University School of Medicine

See next page for additional authors

Follow this and additional works at: https://scholarworks.smith.edu/nsc_facpubs



Part of the [Neuroscience and Neurobiology Commons](#)

Recommended Citation

Shiu, Fu Hung; Wong, Jennifer C.; Yamamoto, Takahiro; Lala, Trisha; Purcell, Ryan H.; Owino, Sharon; Zhu, Dan; Van Meir, Erwin G.; Hall, Randy A.; and Escayg, Andrew, "Mice Lacking Full Length Adgrb1 (bai1) Exhibit Social Deficits, Increased Seizure Susceptibility, and Altered Brain Development" (2022). Neuroscience: Faculty Publications, Smith College, Northampton, MA. https://scholarworks.smith.edu/nsc_facpubs/51

This Article has been accepted for inclusion in Neuroscience: Faculty Publications by an authorized administrator of Smith ScholarWorks. For more information, please contact scholarworks@smith.edu

Authors

Fu Hung Shiu, Jennifer C. Wong, Takahiro Yamamoto, Trisha Lala, Ryan H. Purcell, Sharon Owino, Dan Zhu, Erwin G. Van Meir, Randy A. Hall, and Andrew Escayg

1 **Mice lacking full length Adgrb1 (Bai1) exhibit social deficits, increased seizure**
2 **susceptibility, and altered brain development**

3

4 Abbreviated title: *Bai1* influences behavior and seizure susceptibility

5

6 Fu Hung Shiu^{a,b}, Jennifer C. Wong^a, Takahiro Yamamoto^c, Trisha Lala^{b,d}, Ryan H. Purcell^e,
7 Sharon Owino^d, Dan Zhu^f, Erwin G. Van Meir^{c,g}, Randy A. Hall^d, Andrew Escayg^{a*}

8

9 ^a Department of Human Genetics, Emory University School of Medicine, Atlanta, GA, USA

10 ^b Neuroscience Graduate Program, Graduate Division of Biological and Biomedical Sciences,
11 Laney Graduate School, Emory University, Atlanta, Georgia, USA

12 ^c Department of Neurosurgery, School of Medicine, University of Alabama at Birmingham (UAB),
13 Birmingham, AL, USA

14 ^d Department of Pharmacology and Chemical Biology, Emory University School of Medicine,
15 Atlanta, GA, USA

16 ^e Department of Cell Biology, Emory University School of Medicine, Atlanta, GA, USA

17 ^f Department of Neurosurgery, Emory University School of Medicine, Atlanta, GA, USA

18 ^g O'Neal Comprehensive Cancer Center, University of Alabama at Birmingham (UAB),
19 Birmingham, AL, USA

20

21

22 * Corresponding author:
23 Andrew Escayg, Ph.D.
24 Email: aescayg@emory.edu
25 Phone number: +1-404-712-8328

26

27

28 **Highlights**

- 29 • BAI1/ADGRB1 is an adhesion GPCR that interacts with autism-relevant proteins.
- 30 • *Adgrb1*^{-/-} mice show deficits in sociability and increased seizure susceptibility.
- 31 • *Adgrb1*^{-/-} mice display reduced brain weight and neuron density.
- 32 • Loss of full length Bai1 is associated with a range of clinically relevant features.

33

34

35 **Abstract**

36 The adhesion G protein-coupled receptor BAI1/ADGRB1 plays an important role in suppressing
37 angiogenesis, mediating phagocytosis, and acting as a brain tumor suppressor. BAI1 is also a
38 critical regulator of dendritic spine and excitatory synapse development and interacts with
39 several autism-relevant proteins. However, little is known about the relationship between altered
40 BAI1 function and clinically relevant phenotypes. Therefore, we studied the effect of reduced
41 expression of full length Bai1 on behavior, seizure susceptibility, and brain morphology in
42 *Adgrb1* mutant mice. We compared homozygous (*Adgrb1*^{-/-}), heterozygous (*Adgrb1*^{+/-}), and wild-
43 type (WT) littermates using a battery of tests to assess social behavior, anxiety, repetitive
44 behavior, locomotor function, and seizure susceptibility. We found that *Adgrb1*^{-/-} mice showed
45 significant social behavior deficits and increased vulnerability to seizures. *Adgrb1*^{-/-} mice also
46 showed delayed growth and reduced brain weight. Furthermore, reduced neuron density and
47 increased apoptosis during brain development were observed in the hippocampus of *Adgrb1*^{-/-}
48 mice, while levels of astrogliosis and microgliosis were comparable to WT littermates. These
49 results show that reduced levels of full length Bai1 is associated with a broader range of
50 clinically relevant phenotypes than previously reported.

51 **Keywords**

52 BAI1, seizures, epilepsy, autism, GPCR

53

54 **Introduction**

55 Brain-specific angiogenesis inhibitor (BAI1/ADGRB1) is a member of the adhesion G protein-
56 coupled receptor (GPCR) family (Duman et al., 2016; Purcell and Hall, 2018). Besides sharing a
57 well-conserved seven-transmembrane structure with other GPCRs, BAI1 also features a large
58 N-terminal extracellular domain with five thrombospondin type 1 repeats (TSRs) and a GPCR-
59 autoproteolysis-inducing (GAIN) domain (Cork and Van Meir, 2011; Stephenson et al., 2014).
60 BAI1 suppresses angiogenesis (Cork et al., 2012; Kaur et al., 2009; Zhu et al., 2012), mediates
61 engulfment of apoptotic cells and gram-negative bacteria (Das et al., 2011; Park et al., 2007;
62 Sokolowski et al., 2011), promotes myogenesis (Hochreiter-Hufford et al., 2013), and serves as
63 a brain tumor suppressor by stabilizing p53 (Zhu et al., 2018). Although BAI1 was first
64 associated with non-neuronal functions, the receptor is most abundantly expressed in neurons
65 and glia in the cortex, hippocampus, thalamus, amygdala, and striatum (Sokolowski et al., 2011;
66 Zhang et al., 2014). *Adgrb1* mRNA expression peaks at postnatal day 10 (P10) in rodents and
67 expression is maintained into adulthood (Kee et al., 2004).

68 Studies during the past decade indicate that *in vitro* and *in vivo* knockdown of Bai1 leads
69 to the formation of more immature and unstable dendrites (Duman et al., 2019; Duman et al.,
70 2013), while overexpression of Bai1 results in dendrite retraction (Duman et al., 2019). Mice
71 lacking full-length Bai1 display reduced expression of post-synaptic density 95 (PSD-95) (Zhu et
72 al., 2015), a protein that regulates synaptic stability and plasticity (Cheng et al., 2006). The
73 continuous morphological modifications of dendrites and proper PSD-95 function are essential
74 for learning and memory (Coley and Gao, 2018; Migaud et al., 1998) and are often altered in
75 neurodevelopmental and neurological disorders (Lin and Koleske, 2010; Penzes et al., 2011;
76 Tsai et al., 2012), primarily those characterized by impaired social interaction, communication
77 deficits, and repetitive behaviors (D'Hooge and De Deyn, 2001). Consistent with this
78 observation, *Adgrb1*^{-/-} mice exhibit deficits in spatial memory and alterations in synaptic plasticity

79 that are reflected by enhanced long-term potential (LTP) and reduced long-term depression
80 (LTD) (Zhu et al., 2015).

81 *De novo* rare variants in *ADGRB1* have been identified in patients with autism spectrum
82 disorder (ASD) (Satterstrom et al., 2020). A substantial percentage of individuals with ASD (8-
83 24%) have epilepsy and exhibit altered brain morphology and developmental delay (Amiet et al.,
84 2008; Gabis et al., 2005; Ghacibeh and Fields, 2015). These behavioral phenotypes are also
85 seen in animal models of ASD (Sierra-Arregui et al., 2020; Varghese et al., 2017). Furthermore,
86 BAI1 interacts with autism-relevant proteins, including BAIAP2/IRSp53 and Neuroligin-1 (NLG1)
87 (De Rubeis et al., 2014; Nakanishi et al., 2017; Oda et al., 1999), although little is known about
88 the functional significance of these interactions. Therefore, in the current study, we investigated
89 the *in vivo* physiological role of BAI1 by characterizing the behavioral and seizure phenotypes of
90 homozygous mice lacking full-length Bai1 (*Adgrb1*^{-/-}) and heterozygous mice (*Adgrb1*^{+/-}) that
91 express approximately 50% of wildtype levels. Our results indicate that *Adgrb1*^{-/-} mice exhibit
92 impairments in sociability, social discrimination, and increased seizure susceptibility. *Adgrb1*^{-/-}
93 mice also display increased apoptosis during brain development, reduced brain weight, and
94 reduced hippocampal neuron density.

95 **Material and methods**

96 **Animals**

97 The generation and genotyping of mice lacking full-length Bai1 were previously described (Zhu
98 et al., 2015). These mice were engineered with a deletion of exon 2 (where the ATG start codon
99 is located) and fail to express full length Bai1. Heterozygous mutants (*Adgrb1*^{+/-}) on a C57BL/6J
100 (000664, Jackson laboratory) background were bred to generate wildtype (WT), heterozygous
101 (*Adgrb1*^{+/-}), and homozygous (*Adgrb1*^{-/-}) offspring. Mice were housed in groups of 3-5 on a 12-
102 hour light/dark cycle with standard laboratory rodent chow (5001, Lab Diet) and water available

103 *ad libitum*. All experiments were performed in accordance with the Emory University Institutional
104 Animal Care and Use Committee (IACUC) guidelines.

105 **Survival and body growth curve analysis**

106 Male and female *Adgrb1^{-/-}*, *Adgrb1^{+/-}* and WT littermates were weighed once every two days
107 from postnatal day 7 to 24 (P7 – P24) and then once a week until P65 (n=9-15/group).

108 **Brain weight assessment**

109 Male and female mice of all genotypes at three different ages (P1, 3 week, 2-3 month) were
110 weighed and anesthetized with isoflurane. Brains were harvested and immediately weighed
111 (n=8-18/group).

112 **Immunofluorescence staining and imaging**

113 Brains were postfixed in 4% PFA overnight at 4°C and then transferred to 30% sucrose solution
114 in phosphate-buffered saline (PBS). Coronal sections (40 µm) were stained using with
115 antibodies against GFAP (1:400, 13-0300, Thermo Fischer Scientific), IBA1 (1:400, Ab178846,
116 Abcam), NeuN (1:1000, MAB377, Millipore), and cleaved-caspase-3 (CC3) (1:200, 9664, Cell
117 signaling Technology). Goat anti-mouse IgG (1:500, ab150114, Abcam) and goat anti-Rat IgG
118 (1:500, A-21434, Thermo Fischer) were used as the secondary antibodies for NeuN and GFAP,
119 respectively. Goat anti-rabbit IgG (1:500, ab150077, Abcam) was used as the secondary
120 antibody for IBA1 and CC3. Slides were washed multiple times with PBS and incubated with
121 appropriate fluorescently labeled secondary antibodies for 1 h at 37°C. For NeuN, GFAP, and
122 IBA1 staining, confocal images were acquired on an Olympus FV1000 inverted microscope
123 using the Olympus Fluoview v4.2 software. For CC3 staining, an upright microscope (DM6000B
124 Leica) was used. Three sections per mouse containing the hippocampus and primary
125 somatosensory cortex (bregma –1.96 mm) were used for immunofluorescence staining. NeuN
126 positive cells in the dentate gyrus (DG) and CA1 were counted per mm². CC3 positive (CC3+)
127 cells were counted in the DG, CA1, and primary somatosensory cortex. GFAP and IBA1

128 immunoreactivity (IR) was calculated as the percentage area of the total region of interest (ROI)
129 of the DG and CA1 using ImageJ. A threshold for IR was determined across all antibody images
130 as previously described (Chalermphanupap et al., 2018). The IR area within the ROI and the
131 total area of the ROI were calculated using the "Measure" feature of ImageJ, and the
132 percentage area of IR was determined (area of IR within ROI divided by the total area of ROI
133 and multiplied by 100). Two sections per mouse containing the rostral hippocampus were used
134 for P1 mice. Similarly, CC3+ cells were counted in the DG, CA1, and primary somatosensory
135 cortex. The experimenter was blinded to genotype during quantification.

136 **Western Blot**

137 Whole brain was dissected from 5 month old WT, *Adgrb1^{+/-}*, and, *Adgrb1^{-/-}* littermates, and the
138 left hemisphere was used for western blot. Tissue extracts were prepared in RIPA buffer
139 (89901, Thermo) containing protease and phosphatase inhibitor mix (1861280, Thermo), and
140 total protein was quantified using the BCA protein assay. Laemmli sample buffer (1610747,
141 BIORAD) was added after the BCA protein assay. Protein samples (75 µg) were loaded without
142 boiling on a 10 % SDS-PAGE gel, resolved at 100 V/cm for 2.5 hours, and transferred to a
143 PVDF membrane (1620177, BIORAD). Membranes were blocked with 5 % milk and incubated
144 overnight at 4 °C with an anti C-terminal BAI1 antibody (1:1000, AP8170a, Abcepta; epitope:
145 amino acids 1537-1567), followed by an anti-rabbit HRP-conjugated secondary antibody
146 (1:5000; 31460, Thermo Fischer). The intensity of the Bai1 band was quantified using ImageJ
147 (NIH) as previously described (Zhu et al., 2018) (n=3/genotype).

148 **Behavioral analysis**

149 Behavioral analysis was performed on 3-5 month old male *Adgrb1^{-/-}*, *Adgrb1^{+/-}*, and WT
150 littermates. All behavioral assessments were videotaped and scored using the ANY-Maze Video
151 Tracking System (Stoelting Co.) by an experimenter blinded to genotype. Behavioral analyses

152 were conducted one week apart in the following order: open field, novel object recognition,
153 novel cage, and three-chamber social interaction.

154 **Open field and novel object recognition**

155 Novel object recognition was performed over 4 days as previously described (Dutton et al.,
156 2017; Sawyer et al., 2016; Wong et al., 2021a; Wong et al., 2018). The apparatus consisted of
157 an arena with opaque Plexiglas walls (60 cm x 60 cm x 60 cm). The center zone was a 30 cm x
158 30 cm area in the center of the chamber. On day 1, each mouse was placed in the empty arena
159 and allowed to explore for 10 min. Locomotor activity, total distance traveled, average speed,
160 and time spent in the center zone were scored. On days 2 and 3, two identical objects (cube or
161 sphere) were placed in the center of the arena, and each mouse explored the arena for 10 min
162 (n=13/genotype). On day 4, one of the objects was replaced with a novel object (cube was
163 replaced with the sphere or vice versa). The objects and the location of the novel versus familiar
164 object were counterbalanced. The time spent exploring each object was used to calculate a
165 discrimination ratio (time exploring the novel object/ (time exploring the novel object + time
166 exploring the familiar object) (n=7-8/genotype).

167 **Three-chamber social interaction**

168 Sociability and social discrimination were examined using the three-chamber social interaction
169 paradigm (Dutton et al., 2017; Sawyer et al., 2016; Wong et al., 2021b). A partition separated
170 each chamber (20 cm x 40 cm x 20 cm) with an opening to allow the mouse to move freely
171 between them. The experiment consisted of three 10-minute sessions. The test mouse was first
172 placed in the center chamber, with an empty cylindrical wire cage in the left and right chambers,
173 and the mouse was allowed to freely explore for 10 minutes. In the second 10-minute session,
174 an age- and sex-matched C57BL/6J mouse (stranger) was placed under one of the wire cages
175 while the wire cage on the opposite side remained empty (object). The test mouse was again
176 placed in the center chamber and allowed to explore freely. Time interacting with the 'stranger'

177 mouse vs. the empty cage was calculated as a measure of 'sociability'. For the third 10-minute
178 session, a second age- and sex-matched C57BL/6J mouse (novel mouse) was placed under
179 the previously empty wire cage. The test mouse was again placed in the center chamber and
180 allowed to explore freely. Time interacting with either the first (now 'familiar') mouse from the
181 second session or the novel mouse introduced in the third session was calculated as a measure
182 of 'social discrimination' (n=7-8/genotype).

183

184 **Novel cage**

185 Each mouse was placed into a novel standard mouse cage (33 cm × 18 cm × 15 cm) and
186 observed for stereotyped behaviors for 10 minutes. The time spent grooming, digging, rearing,
187 and circling was recorded (n=13/genotype).

188

189 **Nestlet shredding**

190 Nesting behavior was performed as previously described (Lustberg et al., 2020). Each mouse
191 was placed into a novel standard mouse cage with a cotton nestlet square (5 cm × 5 cm,
192 approximately 3 g). Nestlets were weighted before the experiment to calculate the percent
193 shredded at the end of the task. Mice were left undisturbed between 1 pm and 3 pm, after which
194 they were returned to their home cages. The weight of the remaining non-shredded nestlet
195 material was recorded (n=13/genotype).

196

197 **Buried food Test**

198 Olfactory function was examined using the buried food test as previously described (Yang and
199 Crawley, 2009). Two days prior to assessment of olfactory function, chocolate-flavored pellets
200 (F05472-1, Bio-Serv) were introduced into the home cage to habituate animals to the novel but

201 highly palatable stimulus. Twenty-four hours prior to behavioral testing, all standard mouse
202 chow and chocolate pellets were removed from the home cage. Mice were tested in the same
203 room in which they were housed. On test day, chocolate pellets were placed in a randomly-
204 selected corner of a clean mouse cage and buried under 3 cm of standard bedding. The latency
205 for the mouse to find and eat (grasp and bite) the chocolate pellets was recorded. Mice that did
206 not feed within 15 min were assigned a maximum feeding latency score of 900 s
207 (n=13/genotype).

208

209 **Seizure induction**

210 Susceptibility to induced seizures was tested in 3-5 month old male and female *Adgrb1*^{-/-},
211 *Adgrb1*^{+/-}, and WT littermates.

212 **6 Hz induced seizures**

213 6 Hz psychomotor seizures were induced as previously described (Giddens et al., 2017;
214 Shapiro et al., 2021; Wong et al., 2016; Wong et al., 2021b). Mice were given a topical
215 analgesic to the cornea (0.5% tetracaine hydrochloride) before stimulation. Corneal electrical
216 stimulation (6 Hz, 3 sec, 17 mA for male and 13 mA for female) was applied through a constant
217 current device (ECT Unit 57800; Ugo Basile), and the mouse was moved immediately into a
218 clean cage for behavioral seizure observation. Resulting seizures were scored on a modified
219 Racine scale: RS0 = no abnormal behavior; RS1 = immobile ≥ 3 sec, RS2 = forelimb clonus,
220 paw waving, RS3 = rearing and falling (n=9-11/group).

221 **Flurothyl induced seizures**

222 Seizure induction using flurothyl was performed as previously described (Martin et al., 2007;
223 Shapiro et al., 2021; Shapiro et al., 2019; Wong et al., 2021a). Each mouse was placed in a
224 plexiglass chamber (34 cm x 20 cm x 15 cm and exposed to flurothyl (bis[2,2,2-trifluoroethyl]

225 ether, 287571-5G, Sigma-Aldrich) at a rate of 20 μ L/min. Latencies to the first myoclonic jerk
226 (MJ) and generalized tonic-clonic seizure (GTCS) were recorded (n=8-11/group).

227 **Statistical analysis**

228 Prism v8.1.2 software (GraphPad) was used for statistical analyses. A 2-way ANOVA followed
229 by Sidak's multiple comparisons test was used to compare the bodyweight of each genotype at
230 the different time points of the growth curve, the time spent interacting with the stranger mouse
231 and novel mouse, total entries into each side chamber during the three-chamber social
232 interaction task, and brain/body weight measurements. For novel object recognition, a one-
233 sample parametric t-test was used to compare the time spent with the novel object against 50%
234 chance. A 1-way ANOVA followed by Tukey's multiple comparisons test was used to analyze
235 the total distance traveled, speed, total time spent in the center of the open field, the latency to
236 the MJ and GTCS during flurothyl seizure induction, the amount of nestlet shredded, the latency
237 to grasp and bite the chocolate pellets in the buried food test, latencies to the first interactions in
238 the three-chamber social interaction task, and immunofluorescence data. For the 6 Hz seizure
239 induction paradigm, an unpaired nonparametric Mann-Whitney U-test was used to compare
240 Racine scores between each genotype. Male and female mice were analyzed separately unless
241 stated. All results are presented as mean \pm SEM and a p-value <0.05 was considered
242 significant.

243 **Results**

244 ***Adgrb1*^{-/-} mice show delayed growth and reduced brain weights**

245 Western blot analysis showed that *Adgrb1*^{-/-} mice lack full length Bai1, and *Adgrb1*^{+/-}
246 mutants express approximately 50% of WT levels. (**Supplementary Fig. 1A-B**). We next
247 examined the developmental profile of *Adgrb1* mutants. We observed that *Adgrb1*^{-/-} mice
248 weighed significantly less than their WT littermates beginning at P15 for males (p=0.0097)
249 (**Supplementary Fig. 2A**) and P9 for females (p=0.0112) (**Supplementary Fig. 2B**); however,

250 by P37, the body weights of *Adgrb1*^{-/-} mice were comparable to same-sex WT littermates. In
251 contrast, there were no significant differences in average body weights between *Adgrb1*^{+/-} and
252 WT littermates at any age.

253 As *Bai1* is highly expressed in brain, we next focused on brain development. We
 254 compared brain weights of male and female mice with each genotype at three time points: P1, 3
 255 weeks, and 2-3 months (**Fig. 1**). At P1, no significant differences were observed in either brain

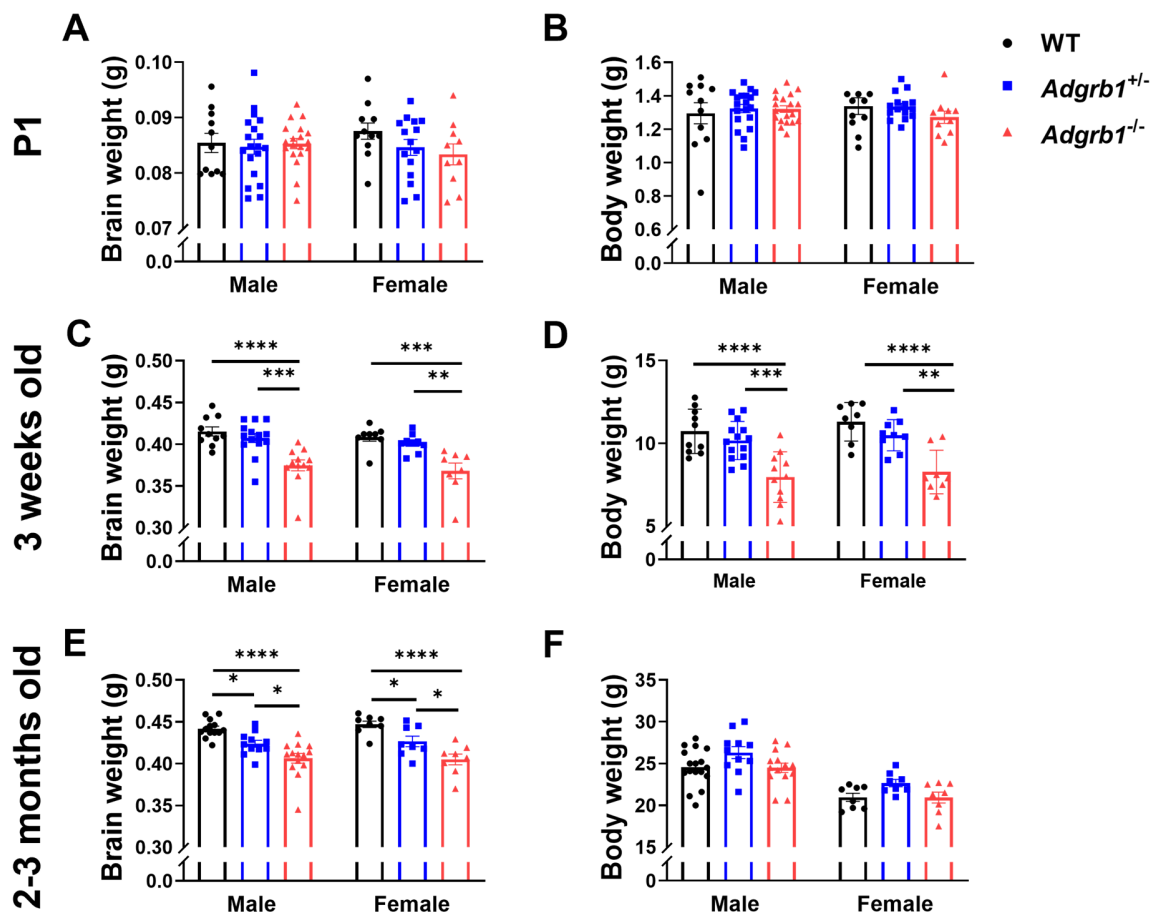


Figure 1. *Adgrb1*^{-/-} mice exhibit reduced brain and body weight. (A-B). *Adgrb1*^{-/-} male and female mice (P1) had comparable brain (A) and body weights (B). Male: WT, n = 11; *Adgrb1*^{+/-}, n = 19; *Adgrb1*^{-/-}, n = 19, Female: WT, n = 10; *Adgrb1*^{+/-}, n = 15; *Adgrb1*^{-/-}, n = 10. (C-D). *Adgrb1*^{-/-} male and female mice (3 weeks old) had lower average brain (C) and body weights (D) compared to same-sex *Adgrb1*^{+/-} mutants and WT littermates. Male: WT, n = 10; *Adgrb1*^{+/-}, n = 14; *Adgrb1*^{-/-}, n = 12, Female: WT, n = 8; *Adgrb1*^{+/-}, n = 9; *Adgrb1*^{-/-}, n = 8. (E) *Adgrb1*^{-/-} and *Adgrb1*^{+/-} male and female mice (2-3 months old) had lower average brain weights compared to WT littermates. (F) Body weights were comparable in 2–3 month old mice across all three genotypes. Male: WT, n = 14; *Adgrb1*^{+/-}, n = 11; *Adgrb1*^{-/-}, n = 14, Female: WT, n = 8; *Adgrb1*^{+/-}, n = 8; *Adgrb1*^{-/-}, n = 9. Mean ± SEM. **p*<0.05, ***p*<0.01, ****p*<0.001, *****p*<0.0001.

256 (p=0.3326) or body weight (p=0.6) (Fig. 1A-B). However, at 3 weeks of age, average brain
 257 weights of *Adgrb1*^{-/-} mice of both sexes were significantly less than sex-matched *Adgrb1*^{+/-} and
 258 WT littermates (p<0.001) (Fig. 1C). The average body weight of *Adgrb1*^{-/-} mice was also
 259 significantly less than sex-matched *Adgrb1*^{+/-} mice and WT littermates (p=0.0107) (Fig. 1D). At
 260 2-3 months of age, no significant differences in average body weights between same-sex mice
 261 across all three genotypes were found (p=0.998) (Fig. 1F); however, average brain weights of
 262 *Adgrb1*^{-/-} mice of both sexes were significantly less than same-sex *Adgrb1*^{+/-} mice and WT
 263 littermates (p<0.0001) (Fig. 1E). In contrast to the other time points, at 2-3 months of age, the
 264 average brain weight of *Adgrb1*^{-/-} mice was significantly lower than same-sex WT littermates
 265 (p<0.05) (Fig. 1E).

266 **2-3 month old *Adgrb1*^{-/-} mice exhibit reduced neuron density in the dentate gyrus and**
 267 **CA1**

268 Since brain weight was lower in 2-3 month old *Adgrb1*^{-/-} mice, we next examined whether brain
 269 morphology was altered. We focused on the hippocampus since *Adgrb1*^{-/-} mice were previously
 270 shown to exhibit altered hippocampal LTP and LTD, and deficits in hippocampal dependent
 271 spatial memory (Zhu et al., 2015). We quantified neuron density in 2–3 month old male mice of
 272 each genotype in two hippocampal regions: the dentate gyrus (DG) and CA1. *Adgrb1*^{-/-} male
 273 mice displayed significantly lower neuron density in both the DG (p=0.0402) (Fig. 2A-D) and

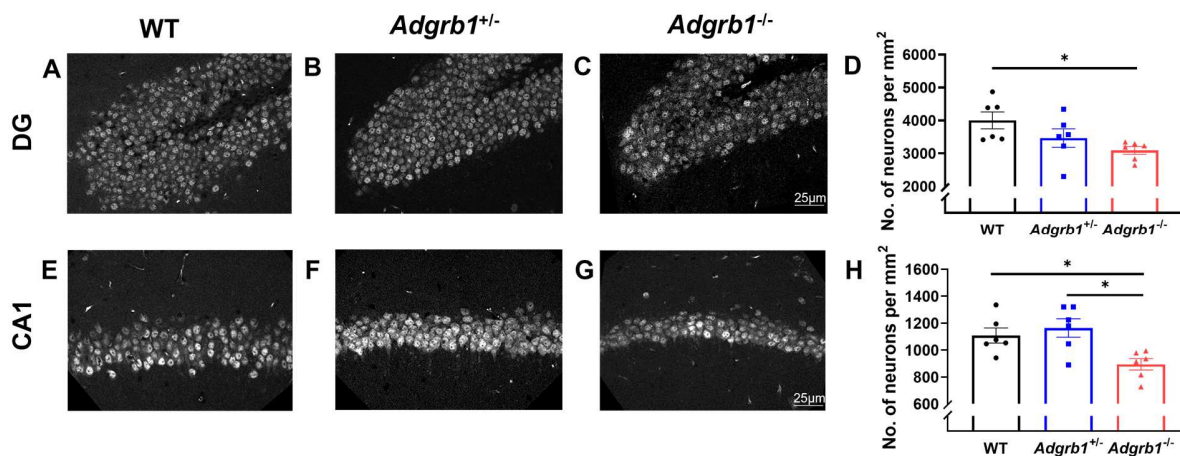


Figure 2. Reduced neuron density in 2-3 month old *Adgrb1*^{-/-} mice. Representative images of NeuN positive cells in the DG (A-C) and CA1 region (E-G). *Adgrb1*^{-/-} mice had significantly lower neuron density in the DG (D) and CA1 (H) than *Adgrb1*^{+/-} and WT littermates. WT, n = 6; *Adgrb1*^{+/-}, n = 6; *Adgrb1*^{-/-}, n = 6. Mean ± SEM. *p<0.05.

274 CA1 (p=0.0103) (Fig. 2E-H) compared to WT littermates. We also compared the levels of GFAP
 275 (astrocyte marker) and IBA1 (microglia marker) expression in the DG and CA1 between male
 276 mice of each genotype (2-3 months old), and observed no significant differences (p>0.05)
 277 (Supplementary Fig. 3).

278 ***Adgrb1*^{-/-} mice exhibit higher levels of cleaved caspase-3-positive cells in the**
 279 **hippocampal CA1 and primary somatosensory cortex during early postnatal**
 280 **development**

281 To determine whether the reduced neuron density observed in *Adgrb1*^{-/-} mice was associated
 282 with a higher level of apoptosis, we used the cleaved caspase-3 antibody (Porter and Janicke,
 283 1999) to compare apoptosis levels in all three genotypes at P1, 3 weeks, and 2-3 months of
 284 age. As expected, levels of cleaved caspase-3-positive (CC3+) cells were higher in P1 mice
 285 compared to 3 week old and 2-3 month old mice due to the greater level of programmed cell
 286 death (PCD) during early neurodevelopment (Yamaguchi and Miura, 2015). At P1, comparable
 287 levels CC3+ cells were observed in the DG of *Adgrb1*^{-/-} mice and WT littermates (p=0.6801)

288 (Fig. 3A-D); however, we observed a significantly greater number of CC3+ cells in the CA1
 289 region of *Adgrb1*^{-/-} mice (p=0.0186) (Fig. 3E-H). No significant differences were detected
 290 between *Adgrb1*^{+/-} mice and WT littermates. We also examined CC3+ cell levels in the primary
 291 somatosensory cortex, a region in which Bai1 is also highly expressed (Sokolowski et al., 2011).
 292 Similarly, we observed a greater number of CC3+ cells in the somatosensory cortex of P1

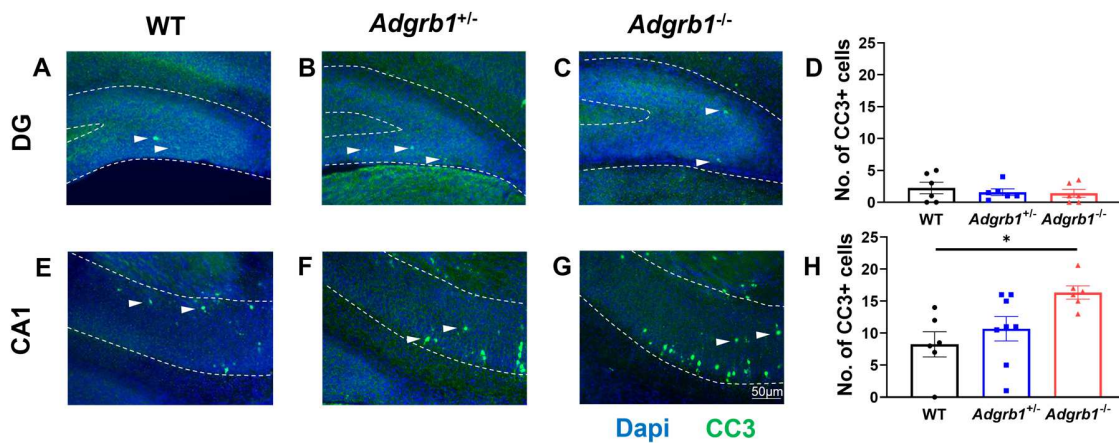


Figure 3. P1 *Adgrb1*^{-/-} mice have more of CC3+ cells in the CA1. (A-C) Representative images of CC3+ cells in the DG. (D) Comparable numbers of CC3+ cells in the DG were observed across all three genotypes. (E-G) Representative images of CC3+ cells in the CA1. (H) *Adgrb1*^{-/-} mice had more CC3+ cells in the CA1 than WT littermates. Dashed lines show the boundaries of the DG and CA1 regions. Examples of CC3+ cells are indicated with arrows. Mean ± SEM. WT, n = 6; *Adgrb1*^{+/-}, n = 6; *Adgrb1*^{-/-}, n = 6. *p<0.05.

293 *Adgrb1*^{-/-} mice compared to WT littermates (p=0.023) (Supplementary Fig. 4). Comparable
 294 levels of CC3+ cells were observed in the CA1, DG, and primary somatosensory cortex of 3
 295 week old and 2–3 month old mice of each genotype (Supplementary Fig. 5).

296

297 *Adgrb1*^{-/-} mice exhibit deficits in social behavior and learning and memory

298 We used the three-chamber social interaction paradigm to examine sociability and social
 299 discrimination as BAI1 interacts with the autism relevant proteins, NLG1 and IRSp53, and mice
 300 lacking Nlg1 or Irsps53 show altered social behavior (Blundell et al., 2010; Chung et al., 2015).

301 WT littermates and *Adgrb1*^{+/-} mice spent significantly more time exploring the stranger mouse
302 than the empty cage (p=0.0008 for WT littermates, p=0.0099 for *Adgrb1*^{+/-} mice). In contrast,
303 *Adgrb1*^{-/-} mice did not discriminate between the stranger mouse and empty cage (p=0.6627),
304 suggesting a deficit in sociability (**Fig. 4A**). When presented with the choice between interacting
305 with a novel or familiar mouse, WT littermates showed a significant preference for the novel
306 mouse compared to the familiar mouse (p=0.0097). In contrast, *Adgrb1*^{+/-} and *Adgrb1*^{-/-} mice did

307 not show a statistically significant preference for the novel mouse (*Adgrb1*^{+/-}, $p=0.0984$; *Adgrb1*^{-/-}
 308 , $p=0.7451$), suggesting a deficit in social discrimination (**Fig. 4B**). There were no differences in
 309 total entries into each side chamber, or the latencies to the first interaction with the stranger
 310 mouse or the novel mouse in the ‘sociability’ and ‘social discrimination’ components of the task,
 311 respectively (**Supplementary Fig. 6**). The similar performance of the mice of all three
 312 genotypes in the buried food test (**Fig. 4C**) demonstrates that the observed impairment in social

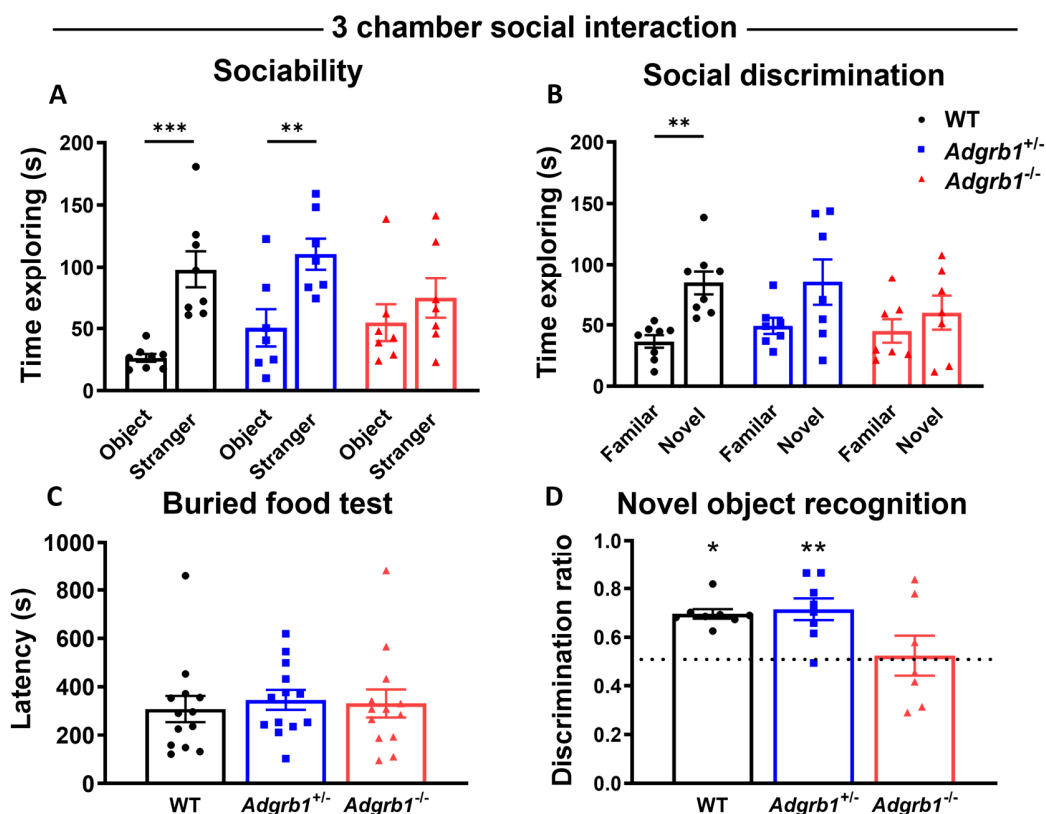


Figure 4. Male *Adgrb1*^{-/-} mice exhibit deficits in sociability, social discrimination, and novel object recognition. (A) *Adgrb1*^{-/-} mice did not significantly discriminate between a stranger mouse and an empty cage, demonstrating a sociability deficit. (B) *Adgrb1*^{+/-} and *Adgrb1*^{-/-} mutants did not exhibit a significant preference for a novel vs. a familiar mouse, indicating a deficit in social discrimination. WT, $n = 8$; *Adgrb1*^{+/-}, $n = 8$; *Adgrb1*^{-/-}, $n = 7$. (C) *Adgrb1*^{-/-} mice spent similar amount of time to find buried food. WT, $n = 13$; *Adgrb1*^{+/-}, $n = 13$; *Adgrb1*^{-/-}, $n = 13$ (D) *Adgrb1*^{-/-} mice did not discriminate between the novel and familiar object, suggesting a deficit in long-term recognition memory. WT, $n = 8$; *Adgrb1*^{+/-}, $n = 8$; *Adgrb1*^{-/-}, $n = 7$. Mean \pm SEM. * $p < 0.05$, ** $p < 0.01$, *** $p < 0.001$.

313 interaction is unlikely to be due to olfactory dysfunction.

314 In addition to abnormalities in social behavior, deficits in learning and memory have
315 been described in patients and animal models of ASD (Pasciuto et al., 2015; Silverman et al.,
316 2010). Therefore, we used the novel object recognition task to examine long-term recognition
317 memory. WT littermates and *Adgrb1*^{+/-} mice spent significantly more time exploring the novel
318 object compared to 50% chance (WT, $p < 0.0001$; *Adgrb1*^{+/-}, $p = 0.0019$) (**Fig. 4D**). In contrast,
319 *Adgrb1*^{-/-} mice did not show a significant preference for the novel object ($p = 0.7765$), suggesting
320 a deficit in long-term recognition memory.

321 We also subjected the mice to the open field paradigm to examine locomotor activity and
322 anxiety-like behaviors. Distance traveled ($p = 0.187$) (**Supplementary Fig. 7A**) and average
323 speed ($p = 0.1865$) (**Supplementary Fig. 7B**) were found to be comparable between the three
324 genotypes. *Adgrb1*^{-/-} mice spent more time than WT littermates in the center of the open field
325 ($p = 0.012$), suggesting that loss of full length Bai1 is not associated with increased anxiety-like
326 behavior (**Supplementary Fig. 7C**). Lastly, we examined nesting behavior (**Supplementary**
327 **Fig. 7D**) and stereotypical behaviors (**Supplementary Fig. 7E**) and found that all three
328 genotypes performed similarly ($p = 0.294$ and 0.328 , respectively).

329 ***Adgrb1*^{-/-} mice are susceptible to induced seizures**

330 Along with social deficits, many mouse models of ASD exhibit an increased vulnerability to
331 seizures, an observation that is consistent with clinical observations that epilepsy is often
332 comorbid with ASD (Ghacibeh and Fields, 2015; Hughes and Melyn, 2005). Therefore, we
333 explored whether *Adgrb1* mutants might exhibit alterations in seizure susceptibility. In the 6 Hz
334 paradigm, seizures were observed in all *Adgrb1*^{-/-} mice (male: 3 RS1, 7 RS2; $p = 0.0185$, female:
335 6 RS2, 2 RS3; $p = 0.0039$) (**Fig. 5A and D**). In contrast, only 25% and 33% of male and female
336 WT littermates seized, respectively (male: 6 RS0, 2 RS2; female: 6 RS0, 3 RS2). Additionally,
337 when exposed to the proconvulsant flurothyl, *Adgrb1*^{-/-} mutants displayed shorter average

338 latencies to the first myoclonic jerk (MJ) (male, $p < 0.0001$; female, $p = 0.0002$) (**Fig. 5B and E**)
 339 and generalized tonic-clonic seizure (GTCS) (male, $p = 0.0004$; female, $p = 0.0014$) when

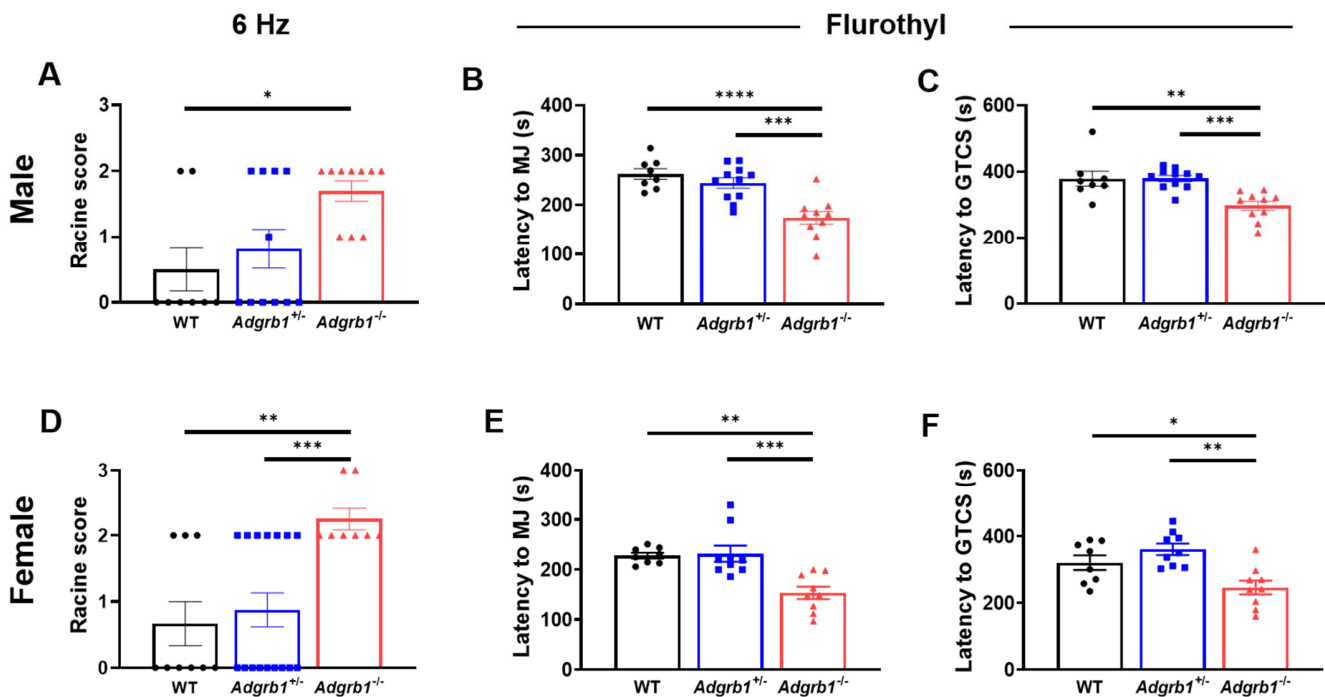


Figure 5. *Adgrb1*^{-/-} mice are susceptible to induced seizures. (A and D) *Adgrb1*^{-/-} male and female mice were more susceptible to 6 Hz seizures when compared to *Adgrb1*^{+/-} and WT littermates. Male: WT, n = 8; *Adgrb1*^{+/-}, n = 11; *Adgrb1*^{-/-}, n = 10, Female: WT, n = 9; *Adgrb1*^{+/-}, n = 18, *Adgrb1*^{-/-}, n = 8. (B and E) *Adgrb1*^{-/-} male and female mutants exhibited shorter latencies to the flurothyl-induced myoclonic jerk (MJ) and (C and F) the first generalized tonic-clonic seizure (GTCS) compared to *Adgrb1*^{+/-} and WT littermates. Male: WT, n = 8; *Adgrb1*^{+/-}, n = 11; *Adgrb1*^{-/-}, n = 10, Female: WT, n = 8; *Adgrb1*^{+/-}, n = 9; *Adgrb1*^{-/-}, n = 9. Mean \pm SEM. * $p < 0.05$, ** $p < 0.01$, *** $p < 0.001$, **** $p < 0.0001$.

340 compared to same-sex WT littermates (**Fig. 5C and F**). In contrast, there were no differences in
 341 the average latency to the MJ or GTCS between same-sex heterozygous mutants and WT
 342 littermates.

343 Discussion

344 In the current study, we identified a wide range of phenotypes, including delayed growth,
 345 reduced brain weight, higher levels of apoptosis, deficits in social behavior, and increased

346 seizure susceptibility in mice lacking full length Bai1 expression. These observations expand the
347 clinical features that could be potentially associated with BAI1 dysfunction.

348 We found that 3 week old *Adgrb1*^{-/-} mice weighed significantly less than *Adgrb1*^{+/-} and
349 WT littermates; however, body weight was comparable between genotypes at 2-3 months of
350 age. Lower body weight during early development has been previously reported for several
351 mouse models of autism (Portmann et al., 2014; Yang et al., 2016). It is possible that
352 competition with the WT littermates prior to weaning could have reduced milk intake in the
353 mutants, thereby contributing to the slower initial weight gain. In contrast, at both the 3 week
354 and 2–3 month time points, the average brain weight of *Adgrb1*^{-/-} mutants was significantly less
355 than WT littermates. Thus, the lower brain weight in *Adgrb1*^{-/-} mutants was not simply due to the
356 overall smaller size of the mutant mice. Consistent with the lower brain weights, we observed
357 reduced neuron density in the DG and CA1 regions of 2-3 month old *Adgrb1*^{-/-} mice. Since Bai1
358 is known to mediate the clearance of apoptotic cells (Mazaheri et al., 2014) (Sokolowski et al.,
359 2011), we speculated that the absence of full-length Bai1 during early brain development may
360 result in increased levels of uncleared apoptotic cells. In turn, this could contribute to secondary
361 necrosis, neuron loss, and lower brain weight (Elliott and Ravichandran, 2010; Glass et al.,
362 2010). In support of this prediction, we observed increased CC3+ cells in the CA1 region and
363 somatosensory cortex of P1 *Adgrb1*^{-/-} mice. Interestingly, the number of CC3+ cells in these
364 regions were comparable between the three genotypes at the 3 week and 2-3 month time
365 points, suggesting that Bai1 might play a greater role in the clearance of apoptotic cells early in
366 brain development, a period that has the highest levels of apoptosis due to programmed cell
367 death (Ahern et al., 2013; Yamaguchi and Miura, 2015).

368 While we observed reduced neuron density in both CA1 and DG of 2-3 month old
369 *Adgrb1*^{-/-} mice, similar levels of CC3+ cells were detected in the DG of P1 *Adgrb1*^{-/-} mice and
370 WT littermates. This suggests reduced clearance of apoptotic cells during early development is

371 unlikely to be solely responsible for the observation of reduced neuron density. Thus, additional
372 studies will be required to fully resolve the underlying mechanisms.

373 Recent sequence analyses of ASD patients identified several *de novo* BAI1 variants
374 (Satterstrom et al., 2020), suggesting that BAI1 might also play a role in ASD. BAI1 also
375 interacts with autism-associated proteins, such as NLG1 and BAIAP2/IRSp53 (Nakanishi et al.,
376 2017; Shiratsuchi et al., 1998; Toma et al., 2011; Tu et al., 2018). *Nlg1*^{-/-} and *Irsp53*^{-/-} mice also
377 show abnormal social behavior, memory deficits, and altered synaptic plasticity (Blundell et al.,
378 2010; Chung et al., 2015; Kim et al., 2009). However, while the phenotypes of *Adgrb1*^{-/-} mutants
379 overlap with *Nlg1*^{-/-} and *Irsp53*^{-/-} mice, the underlying mechanisms for the observed phenotypes
380 might not be identical. Lack of full-length Bai1 leads to rapid degradation of Psd-95 due to the
381 activation of the E3 ubiquitin ligase Mdm2 (Zhu et al., 2015), and mice lacking Psd-95 similarly
382 demonstrate sociability and memory deficits (Coley and Gao, 2019; Migaud et al., 1998).
383 However, no changes in Psd-95 protein levels were reported in *Irsp53*^{-/-} and *Nlg1*^{-/-} mice
384 (Blundell et al., 2010; Kim et al., 2009), indicating other pathways might exist that cause the
385 similar deficits observed in *Nlg1*^{-/-} and *Irsp53*^{-/-} mice.

386 In addition to the memory and social behavior deficits observed in the *Adgrb1* mutants,
387 we also found that these mice are more seizure susceptible. While the mechanistic basis for this
388 observation is currently unknown, it may be due, in part, to disrupted protein-protein
389 interactions. For example, BAI1 interacts with BAI1 associated protein 3 (BAIAP3), which
390 mediates endosome fusion within the trans-Golgi network (Zhang et al., 2017). BAIAP3 can
391 modulate GABAergic neuronal firing (Wojcik et al., 2013), and *Baiap3*^{-/-} mice also exhibit
392 increased seizure susceptibility (Wojcik et al., 2013). Furthermore, *Adgrb1* mutants exhibit
393 enhanced NMDA mediated long-term potential (LTP), which can also be an underlying cause of
394 increased seizure susceptibility (Kapur, 2018).

395 While the alterations in social behavior, seizure susceptibility, and body weight were only
396 observed in homozygous *Adgrb1*^{-/-} mutants, brain weight was reduced in both the *Adgrb1*^{+/-} and
397 *Adgrb1*^{-/-} mutants. These observations demonstrate that Bai1 haploinsufficiency can influence
398 biological processes, and that some disease phenotypes associated with Bai1 dysfunction may
399 be affected by gene dosage. The current study reveals previously undescribed roles for BAI1 in
400 regulating social behavior, seizure vulnerability, and CNS development, thus implicating BAI1 in
401 a range of clinically challenging neurological disorders, including ASD and epilepsy.

402 **Funding sources**

403 This work was supported by the National Institutes of Health (EGVM, CA096236 and
404 NS117666), Emory University Integrated Cellular Imaging Microscopy Core of the Emory
405 Neuroscience NINDS Core Facilities grant (5P30NS055077), and by an Emory Brain Health
406 Center seed grant (EGVM, RAH, AE). The content is solely the responsibility of the authors and
407 does not necessarily reflect the official views of the National Institutes of Health.

408 **Acknowledgements**

409 We would like to thank Laura Fox-Goharoon of the Emory Integrated Cellular Imaging Core,
410 Daniel Lustberg for assisting the buried food test, and the Emory Neuroscience NINDS Core
411 Facilities for support and assistance with confocal imaging. We also thank Dr. Deborah Cook for
412 editorial assistance.

413 **Disclosure of conflict of interests**

414 None of the other authors have any conflict of interest to disclose.

415

416

417 **Reference**

- 418 Ahern, T. H., Krug, S., Carr, A. V., Murray, E. K., Fitzpatrick, E., Bengston, L., McCutcheon, J., De Vries, G.
419 J., Forger, N. G., 2013. Cell death atlas of the postnatal mouse ventral forebrain and
420 hypothalamus: effects of age and sex. *J Comp Neurol.* 521, 2551-69.[https://10.1002/cne.23298](https://doi.org/10.1002/cne.23298).
- 421 Amiet, C., Gourfinkel-An, I., Bouzamondo, A., Tordjman, S., Baulac, M., Lechat, P., Mottron, L., Cohen, D.,
422 2008. Epilepsy in autism is associated with intellectual disability and gender: evidence from a
423 meta-analysis. *Biol Psychiatry.* 64, 577-82.[https://10.1016/j.biopsych.2008.04.030](https://doi.org/10.1016/j.biopsych.2008.04.030).
- 424 Blundell, J., Blaiss, C. A., Etherton, M. R., Espinosa, F., Tabuchi, K., Walz, C., Bolliger, M. F., Sudhof, T. C.,
425 Powell, C. M., 2010. Neuroligin-1 deletion results in impaired spatial memory and increased
426 repetitive behavior. *J Neurosci.* 30, 2115-29.[https://10.1523/JNEUROSCI.4517-09.2010](https://doi.org/10.1523/JNEUROSCI.4517-09.2010).
- 427 Chalermpananupap, T., Schroeder, J. P., Rorabaugh, J. M., Liles, L. C., Lah, J. J., Levey, A. I., Weinschenker,
428 D., 2018. Locus Coeruleus Ablation Exacerbates Cognitive Deficits, Neuropathology, and
429 Lethality in P301S Tau Transgenic Mice. *J Neurosci.* 38, 74-92.[https://10.1523/JNEUROSCI.1483-](https://doi.org/10.1523/JNEUROSCI.1483-17.2017)
430 [17.2017](https://doi.org/10.1523/JNEUROSCI.1483-17.2017).
- 431 Cheng, D., Hoogenraad, C. C., Rush, J., Ramm, E., Schlager, M. A., Duong, D. M., Xu, P., Wijayawardana,
432 S. R., Hanfelt, J., Nakagawa, T., Sheng, M., Peng, J., 2006. Relative and absolute quantification of
433 postsynaptic density proteome isolated from rat forebrain and cerebellum. *Mol Cell Proteomics.*
434 5, 1158-70.[https://10.1074/mcp.D500009-MCP200](https://doi.org/10.1074/mcp.D500009-MCP200).
- 435 Chung, W., Choi, S. Y., Lee, E., Park, H., Kang, J., Park, H., Choi, Y., Lee, D., Park, S. G., Kim, R., Cho, Y. S.,
436 Choi, J., Kim, M. H., Lee, J. W., Lee, S., Rhim, I., Jung, M. W., Kim, D., Bae, Y. C., Kim, E., 2015.
437 Social deficits in IRSp53 mutant mice improved by NMDAR and mGluR5 suppression. *Nat*
438 *Neurosci.* 18, 435-43.[https://10.1038/nn.3927](https://doi.org/10.1038/nn.3927).
- 439 Coley, A. A., Gao, W. J., 2018. PSD95: A synaptic protein implicated in schizophrenia or autism? *Prog*
440 *Neuropsychopharmacol Biol Psychiatry.* 82, 187-194.[https://10.1016/j.pnpbp.2017.11.016](https://doi.org/10.1016/j.pnpbp.2017.11.016).
- 441 Coley, A. A., Gao, W. J., 2019. PSD-95 deficiency disrupts PFC-associated function and behavior during
442 neurodevelopment. *Sci Rep.* 9, 9486.[https://10.1038/s41598-019-45971-w](https://doi.org/10.1038/s41598-019-45971-w).
- 443 Cork, S. M., Kaur, B., Devi, N. S., Cooper, L., Saltz, J. H., Sandberg, E. M., Kaluz, S., Van Meir, E. G., 2012. A
444 proprotein convertase/MMP-14 proteolytic cascade releases a novel 40 kDa vasculostatin from
445 tumor suppressor BAI1. *Oncogene.* 31, 5144-52.[https://10.1038/onc.2012.1](https://doi.org/10.1038/onc.2012.1).
- 446 Cork, S. M., Van Meir, E. G., 2011. Emerging roles for the BAI1 protein family in the regulation of
447 phagocytosis, synaptogenesis, neurovasculature, and tumor development. *J Mol Med (Berl).* 89,
448 743-52.[https://10.1007/s00109-011-0759-x](https://doi.org/10.1007/s00109-011-0759-x).
- 449 D'Hooge, R., De Deyn, P. P., 2001. Applications of the Morris water maze in the study of learning and
450 memory. *Brain Res Brain Res Rev.* 36, 60-90
- 451 Das, S., Owen, K. A., Ly, K. T., Park, D., Black, S. G., Wilson, J. M., Sifri, C. D., Ravichandran, K. S., Ernst, P.
452 B., Casanova, J. E., 2011. Brain angiogenesis inhibitor 1 (BAI1) is a pattern recognition receptor

453 that mediates macrophage binding and engulfment of Gram-negative bacteria. *Proc Natl Acad*
454 *Sci U S A.* 108, 2136-41.<https://10.1073/pnas.1014775108>.

455 De Rubeis, S., He, X., Goldberg, A. P., Poultney, C. S., Samocha, K., Cicek, A. E., Kou, Y., Liu, L., Fromer,
456 M., Walker, S., Singh, T., Klei, L., Kosmicki, J., Shih-Chen, F., Aleksic, B., Biscaldi, M., Bolton, P. F.,
457 Brownfeld, J. M., Cai, J., Campbell, N. G., Carracedo, A., Chahrouh, M. H., Chiocchetti, A. G.,
458 Coon, H., Crawford, E. L., Curran, S. R., Dawson, G., Duketis, E., Fernandez, B. A., Gallagher, L.,
459 Geller, E., Guter, S. J., Hill, R. S., Ionita-Laza, J., Jimenez Gonzalez, P., Kilpinen, H., Klauck, S. M.,
460 Kolevzon, A., Lee, I., Lei, I., Lei, J., Lehtimaki, T., Lin, C. F., Ma'ayan, A., Marshall, C. R., McInnes,
461 A. L., Neale, B., Owen, M. J., Ozaki, N., Parellada, M., Parr, J. R., Purcell, S., Puura, K.,
462 Rajagopalan, D., Rehnstrom, K., Reichenberg, A., Sabo, A., Sachse, M., Sanders, S. J., Schafer, C.,
463 Schulte-Ruther, M., Skuse, D., Stevens, C., Szatmari, P., Tammimies, K., Valladares, O., Voran, A.,
464 Li-San, W., Weiss, L. A., Willsey, A. J., Yu, T. W., Yuen, R. K., Study, D. D. D., Homozygosity
465 Mapping Collaborative for, A., Consortium, U. K., Cook, E. H., Freitag, C. M., Gill, M., Hultman, C.
466 M., Lehner, T., Palotie, A., Schellenberg, G. D., Sklar, P., State, M. W., Sutcliffe, J. S., Walsh, C. A.,
467 Scherer, S. W., Zwick, M. E., Baret, J. C., Cutler, D. J., Roeder, K., Devlin, B., Daly, M. J.,
468 Buxbaum, J. D., 2014. Synaptic, transcriptional and chromatin genes disrupted in autism. *Nature.*
469 515, 209-15.<https://10.1038/nature13772>.

470 Duman, J. G., Mulherkar, S., Tu, Y. K., Erikson, K. C., Tzeng, C. P., Mavratsas, V. C., Ho, T. S., Tolia, K. F.,
471 2019. The adhesion-GPCR BAI1 shapes dendritic arbors via Bcr-mediated RhoA activation
472 causing late growth arrest. *Elife.* 8.<https://10.7554/eLife.47566>.

473 Duman, J. G., Tu, Y. K., Tolia, K. F., 2016. Emerging Roles of BAI Adhesion-GPCRs in Synapse
474 Development and Plasticity. *Neural Plast.* 2016, 8301737.<https://10.1155/2016/8301737>.

475 Duman, J. G., Tzeng, C. P., Tu, Y. K., Munjal, T., Schwechter, B., Ho, T. S., Tolia, K. F., 2013. The adhesion-
476 GPCR BAI1 regulates synaptogenesis by controlling the recruitment of the Par3/Tiam1 polarity
477 complex to synaptic sites. *J Neurosci.* 33, 6964-78.<https://10.1523/JNEUROSCI.3978-12.2013>.

478 Dutton, S. B. B., Dutt, K., Papale, L. A., Helmers, S., Goldin, A. L., Escayg, A., 2017. Early-life febrile
479 seizures worsen adult phenotypes in *Scn1a* mutants. *Exp Neurol.* 293, 159-
480 171.<https://10.1016/j.expneurol.2017.03.026>.

481 Elliott, M. R., Ravichandran, K. S., 2010. Clearance of apoptotic cells: implications in health and disease. *J*
482 *Cell Biol.* 189, 1059-70.<https://10.1083/jcb.201004096>.

483 Gabis, L., Pomeroy, J., Andriola, M. R., 2005. Autism and epilepsy: cause, consequence, comorbidity, or
484 coincidence? *Epilepsy Behav.* 7, 652-6.<https://10.1016/j.yebeh.2005.08.008>.

485 Ghacibeh, G. A., Fields, C., 2015. Interictal epileptiform activity and autism. *Epilepsy Behav.* 47, 158-
486 62.<https://10.1016/j.yebeh.2015.02.025>.

487 Giddens, M. M., Wong, J. C., Schroeder, J. P., Farrow, E. G., Smith, B. M., Owino, S., Soden, S. E., Meyer,
488 R. C., Saunders, C., LePichon, J. B., Weinschenker, D., Escayg, A., Hall, R. A., 2017. GPR37L1
489 modulates seizure susceptibility: Evidence from mouse studies and analyses of a human
490 GPR37L1 variant. *Neurobiol Dis.* 106, 181-190.<https://10.1016/j.nbd.2017.07.006>.

- 491 Glass, C. K., Saijo, K., Winner, B., Marchetto, M. C., Gage, F. H., 2010. Mechanisms underlying
492 inflammation in neurodegeneration. *Cell*. 140, 918-34.<https://10.1016/j.cell.2010.02.016>.
- 493 Hochreiter-Hufford, A. E., Lee, C. S., Kinchen, J. M., Sokolowski, J. D., Arandjelovic, S., Call, J. A., Klibanov,
494 A. L., Yan, Z., Mandell, J. W., Ravichandran, K. S., 2013. Phosphatidylserine receptor BAI1 and
495 apoptotic cells as new promoters of myoblast fusion. *Nature*. 497, 263-
496 7.<https://10.1038/nature12135>.
- 497 Hughes, J. R., Melyn, M., 2005. EEG and seizures in autistic children and adolescents: further findings
498 with therapeutic implications. *Clin EEG Neurosci*. 36, 15-
499 20.<https://10.1177/155005940503600105>.
- 500 Kapur, J., 2018. Role of NMDA receptors in the pathophysiology and treatment of status epilepticus.
501 *Epilepsia Open*. 3, 165-168.<https://10.1002/epi4.12270>.
- 502 Kaur, B., Cork, S. M., Sandberg, E. M., Devi, N. S., Zhang, Z., Klenotic, P. A., Febbraio, M., Shim, H., Mao,
503 H., Tucker-Burden, C., Silverstein, R. L., Brat, D. J., Olson, J. J., Van Meir, E. G., 2009.
504 Vasculostatin inhibits intracranial glioma growth and negatively regulates in vivo angiogenesis
505 through a CD36-dependent mechanism. *Cancer Res*. 69, 1212-20.[https://10.1158/0008-
506 5472.CAN-08-1166](https://10.1158/0008-5472.CAN-08-1166).
- 507 Kee, H. J., Ahn, K. Y., Choi, K. C., Won Song, J., Heo, T., Jung, S., Kim, J. K., Bae, C. S., Kim, K. K., 2004.
508 Expression of brain-specific angiogenesis inhibitor 3 (BAI3) in normal brain and implications for
509 BAI3 in ischemia-induced brain angiogenesis and malignant glioma. *FEBS Lett*. 569, 307-
510 16.<https://10.1016/j.febslet.2004.06.011>.
- 511 Kim, M. H., Choi, J., Yang, J., Chung, W., Kim, J. H., Paik, S. K., Kim, K., Han, S., Won, H., Bae, Y. S., Cho, S.
512 H., Seo, J., Bae, Y. C., Choi, S. Y., Kim, E., 2009. Enhanced NMDA receptor-mediated synaptic
513 transmission, enhanced long-term potentiation, and impaired learning and memory in mice
514 lacking IRSp53. *J Neurosci*. 29, 1586-95.<https://10.1523/JNEUROSCI.4306-08.2009>.
- 515 Lin, Y. C., Koleske, A. J., 2010. Mechanisms of synapse and dendrite maintenance and their disruption in
516 psychiatric and neurodegenerative disorders. *Annu Rev Neurosci*. 33, 349-
517 78.<https://10.1146/annurev-neuro-060909-153204>.
- 518 Lustberg, D., Iannitelli, A. F., Tillage, R. P., Pruitt, M., Liles, L. C., Weinshenker, D., 2020. Central
519 norepinephrine transmission is required for stress-induced repetitive behavior in two rodent
520 models of obsessive-compulsive disorder. *Psychopharmacology (Berl)*. 237, 1973-
521 1987.<https://10.1007/s00213-020-05512-0>.
- 522 Martin, M. S., Tang, B., Papale, L. A., Yu, F. H., Catterall, W. A., Escayg, A., 2007. The voltage-gated
523 sodium channel Scn8a is a genetic modifier of severe myoclonic epilepsy of infancy. *Hum Mol
524 Genet*. 16, 2892-9.<https://10.1093/hmg/ddm248>.
- 525 Mazaheri, F., Breus, O., Durdu, S., Haas, P., Wittbrodt, J., Gilmour, D., Peri, F., 2014. Distinct roles for
526 BAI1 and TIM-4 in the engulfment of dying neurons by microglia. *Nat Commun*. 5,
527 4046.<https://10.1038/ncomms5046>.

528 Migaud, M., Charlesworth, P., Dempster, M., Webster, L. C., Watabe, A. M., Makhinson, M., He, Y.,
529 Ramsay, M. F., Morris, R. G., Morrison, J. H., O'Dell, T. J., Grant, S. G., 1998. Enhanced long-term
530 potentiation and impaired learning in mice with mutant postsynaptic density-95 protein.
531 *Nature*. 396, 433-9.<https://10.1038/24790>.

532 Nakanishi, M., Nomura, J., Ji, X., Tamada, K., Arai, T., Takahashi, E., Bucan, M., Takumi, T., 2017.
533 Functional significance of rare neuroligin 1 variants found in autism. *PLoS Genet*. 13,
534 e1006940.<https://10.1371/journal.pgen.1006940>.

535 Oda, K., Shiratsuchi, T., Nishimori, H., Inazawa, J., Yoshikawa, H., Taketani, Y., Nakamura, Y., Tokino, T.,
536 1999. Identification of BAIAP2 (BAI-associated protein 2), a novel human homologue of hamster
537 IRSp53, whose SH3 domain interacts with the cytoplasmic domain of BAI1. *Cytogenet Cell*
538 *Genet*. 84, 75-82.<https://10.1159/000015219>.

539 Park, D., Tosello-Tramont, A. C., Elliott, M. R., Lu, M., Haney, L. B., Ma, Z., Klibanov, A. L., Mandell, J. W.,
540 Ravichandran, K. S., 2007. BAI1 is an engulfment receptor for apoptotic cells upstream of the
541 ELMO/Dock180/Rac module. *Nature*. 450, 430-4.<https://10.1038/nature06329>.

542 Pasciuto, E., Borrie, S. C., Kanellopoulos, A. K., Santos, A. R., Cappuyns, E., D'Andrea, L., Pacini, L., Bagni,
543 C., 2015. Autism Spectrum Disorders: Translating human deficits into mouse behavior. *Neurobiol*
544 *Learn Mem*. 124, 71-87.<https://10.1016/j.nlm.2015.07.013>.

545 Penzes, P., Cahill, M. E., Jones, K. A., VanLeeuwen, J. E., Woolfrey, K. M., 2011. Dendritic spine pathology
546 in neuropsychiatric disorders. *Nat Neurosci*. 14, 285-93.<https://10.1038/nn.2741>.

547 Porter, A. G., Janicke, R. U., 1999. Emerging roles of caspase-3 in apoptosis. *Cell Death Differ*. 6, 99-
548 104.<https://10.1038/sj.cdd.4400476>.

549 Portmann, T., Yang, M., Mao, R., Panagiotakos, G., Ellegood, J., Dolen, G., Bader, P. L., Grueter, B. A.,
550 Goold, C., Fisher, E., Clifford, K., Rengarajan, P., Kalikhman, D., Loureiro, D., Saw, N. L., Zhengqui,
551 Z., Miller, M. A., Lerch, J. P., Henkelman, M., Shamloo, M., Malenka, R. C., Crawley, J. N.,
552 Dolmetsch, R. E., 2014. Behavioral abnormalities and circuit defects in the basal ganglia of a
553 mouse model of 16p11.2 deletion syndrome. *Cell Rep*. 7, 1077-
554 1092.<https://10.1016/j.celrep.2014.03.036>.

555 Purcell, R. H., Hall, R. A., 2018. Adhesion G Protein-Coupled Receptors as Drug Targets. *Annu Rev*
556 *Pharmacol Toxicol*. 58, 429-449.<https://10.1146/annurev-pharmtox-010617-052933>.

557 Satterstrom, F. K., Kosmicki, J. A., Wang, J., Breen, M. S., De Rubeis, S., An, J. Y., Peng, M., Collins, R.,
558 Grove, J., Klei, L., Stevens, C., Reichert, J., Mulhern, M. S., Artomov, M., Gerges, S., Sheppard, B.,
559 Xu, X., Bhaduri, A., Norman, U., Brand, H., Schwartz, G., Nguyen, R., Guerrero, E. E., Dias, C.,
560 Autism Sequencing, C., i, P.-B. C., Betancur, C., Cook, E. H., Gallagher, L., Gill, M., Sutcliffe, J. S.,
561 Thurm, A., Zwick, M. E., Borglum, A. D., State, M. W., Cicek, A. E., Talkowski, M. E., Cutler, D. J.,
562 Devlin, B., Sanders, S. J., Roeder, K., Daly, M. J., Buxbaum, J. D., 2020. Large-Scale Exome
563 Sequencing Study Implicates Both Developmental and Functional Changes in the Neurobiology
564 of Autism. *Cell*. 180, 568-584 e23.<https://10.1016/j.cell.2019.12.036>.

565 Sawyer, N. T., Helvig, A. W., Makinson, C. D., Decker, M. J., Neigh, G. N., Escayg, A., 2016. Scn1a
566 dysfunction alters behavior but not the effect of stress on seizure response. *Genes Brain Behav.*
567 15, 335-47.<https://10.1111/gbb.12281>.

568 Shapiro, L., Gado, F., Manera, C., Escayg, A., 2021. Allosteric modulation of the cannabinoid 2 receptor
569 confers seizure resistance in mice. *Neuropharmacology.* 188,
570 108448.<https://10.1016/j.neuropharm.2021.108448>.

571 Shapiro, L., Wong, J. C., Escayg, A., 2019. Reduced cannabinoid 2 receptor activity increases
572 susceptibility to induced seizures in mice. *Epilepsia.* 60, 2359-2369.<https://10.1111/epi.16388>.

573 Shiratsuchi, T., Futamura, M., Oda, K., Nishimori, H., Nakamura, Y., Tokino, T., 1998. Cloning and
574 characterization of BAI-associated protein 1: a PDZ domain-containing protein that interacts
575 with BAI1. *Biochem Biophys Res Commun.* 247, 597-604.<https://10.1006/bbrc.1998.8603>.

576 Sierra-Arregui, T., Llorente, J., Gimenez Minguez, P., Tonnesen, J., Penagarikano, O., 2020.
577 Neurobiological Mechanisms of Autism Spectrum Disorder and Epilepsy, Insights from Animal
578 Models. *Neuroscience.* 445, 69-82.<https://10.1016/j.neuroscience.2020.02.043>.

579 Silverman, J. L., Yang, M., Lord, C., Crawley, J. N., 2010. Behavioural phenotyping assays for mouse
580 models of autism. *Nat Rev Neurosci.* 11, 490-502.<https://10.1038/nrn2851>.

581 Sokolowski, J. D., Nobles, S. L., Heffron, D. S., Park, D., Ravichandran, K. S., Mandell, J. W., 2011. Brain-
582 specific angiogenesis inhibitor-1 expression in astrocytes and neurons: implications for its dual
583 function as an apoptotic engulfment receptor. *Brain Behav Immun.* 25, 915-
584 21.<https://10.1016/j.bbi.2010.09.021>.

585 Stephenson, J. R., Purcell, R. H., Hall, R. A., 2014. The BAI subfamily of adhesion GPCRs: synaptic
586 regulation and beyond. *Trends Pharmacol Sci.* 35, 208-15.<https://10.1016/j.tips.2014.02.002>.

587 Toma, C., Hervas, A., Balmana, N., Vilella, E., Aguilera, F., Cusco, I., del Campo, M., Caballero, R., De
588 Diego-Otero, Y., Ribases, M., Cormand, B., Bayes, M., 2011. Association study of six candidate
589 genes asymmetrically expressed in the two cerebral hemispheres suggests the involvement of
590 BAIAP2 in autism. *J Psychiatr Res.* 45, 280-2.<https://10.1016/j.jpsychires.2010.09.001>.

591 Tsai, N. P., Wilkerson, J. R., Guo, W., Maksimova, M. A., DeMartino, G. N., Cowan, C. W., Huber, K. M.,
592 2012. Multiple autism-linked genes mediate synapse elimination via proteasomal degradation of
593 a synaptic scaffold PSD-95. *Cell.* 151, 1581-94.<https://10.1016/j.cell.2012.11.040>.

594 Tu, Y. K., Duman, J. G., Tolias, K. F., 2018. The Adhesion-GPCR BAI1 Promotes Excitatory Synaptogenesis
595 by Coordinating Bidirectional Trans-synaptic Signaling. *J Neurosci.* 38, 8388-
596 8406.<https://10.1523/JNEUROSCI.3461-17.2018>.

597 Varghese, M., Keshav, N., Jacot-Descombes, S., Warda, T., Wicinski, B., Dickstein, D. L., Harony-Nicolas,
598 H., De Rubeis, S., Drapeau, E., Buxbaum, J. D., Hof, P. R., 2017. Autism spectrum disorder:
599 neuropathology and animal models. *Acta Neuropathol.* 134, 537-566.<https://10.1007/s00401-017-1736-4>.

600

601 Wojcik, S. M., Tantra, M., Stepniak, B., Man, K. N., Muller-Ribbe, K., Begemann, M., Ju, A., Papiol, S.,
602 Ronnenberg, A., Gurvich, A., Shin, Y., Augustin, I., Brose, N., Ehrenreich, H., 2013. Genetic
603 markers of a Munc13 protein family member, BAIAP3, are gender specifically associated with
604 anxiety and benzodiazepine abuse in mice and humans. *Mol Med.* 19, 135-
605 48.<https://10.2119/molmed.2013.00033>.

606 Wong, J. C., Dutton, S. B., Collins, S. D., Schachter, S., Escayg, A., 2016. Huperzine A Provides Robust and
607 Sustained Protection against Induced Seizures in Scn1a Mutant Mice. *Front Pharmacol.* 7,
608 357.<https://10.3389/fphar.2016.00357>.

609 Wong, J. C., Grieco, S. F., Dutt, K., Chen, L., Thelin, J. T., Inglis, G. A. S., Parvin, S., Garraway, S. M., Xu, X.,
610 Goldin, A. L., Escayg, A., 2021a. Autistic-like behavior, spontaneous seizures, and increased
611 neuronal excitability in a Scn8a mouse model.
612 *Neuropsychopharmacology*.<https://10.1038/s41386-021-00985-9>.

613 Wong, J. C., Makinson, C. D., Lamar, T., Cheng, Q., Wingard, J. C., Terwilliger, E. F., Escayg, A., 2018.
614 Selective targeting of Scn8a prevents seizure development in a mouse model of mesial temporal
615 lobe epilepsy. *Sci Rep.* 8, 126.<https://10.1038/s41598-017-17786-0>.

616 Wong, J. C., Shapiro, L., Thelin, J. T., Heaton, E. C., Zaman, R. U., D'Souza, M. J., Murnane, K. S., Escayg,
617 A., 2021b. Nanoparticle encapsulated oxytocin increases resistance to induced seizures and
618 restores social behavior in Scn1a-derived epilepsy. *Neurobiol Dis.* 147,
619 105147.<https://10.1016/j.nbd.2020.105147>.

620 Yamaguchi, Y., Miura, M., 2015. Programmed cell death in neurodevelopment. *Dev Cell.* 32, 478-
621 90.<https://10.1016/j.devcel.2015.01.019>.

622 Yang, E. J., Ahn, S., Lee, K., Mahmood, U., Kim, H. S., 2016. Early Behavioral Abnormalities and Perinatal
623 Alterations of PTEN/AKT Pathway in Valproic Acid Autism Model Mice. *PLoS One.* 11,
624 e0153298.<https://10.1371/journal.pone.0153298>.

625 Yang, M., Crawley, J. N., 2009. Simple behavioral assessment of mouse olfaction. *Curr Protoc Neurosci.*
626 Chapter 8, Unit 8 24.<https://10.1002/0471142301.ns0824s48>.

627 Zhang, X., Jiang, S., Mitok, K. A., Li, L., Attie, A. D., Martin, T. F. J., 2017. BAIAP3, a C2 domain-containing
628 Munc13 protein, controls the fate of dense-core vesicles in neuroendocrine cells. *J Cell Biol.* 216,
629 2151-2166.<https://10.1083/jcb.201702099>.

630 Zhang, Y., Chen, K., Sloan, S. A., Bennett, M. L., Scholze, A. R., O'Keefe, S., Phatnani, H. P., Guarnieri, P.,
631 Caneda, C., Ruderisch, N., Deng, S., Liddelow, S. A., Zhang, C., Daneman, R., Maniatis, T., Barres,
632 B. A., Wu, J. Q., 2014. An RNA-sequencing transcriptome and splicing database of glia, neurons,
633 and vascular cells of the cerebral cortex. *J Neurosci.* 34, 11929-
634 47.<https://10.1523/JNEUROSCI.1860-14.2014>.

635 Zhu, D., Li, C., Swanson, A. M., Villalba, R. M., Guo, J., Zhang, Z., Matheny, S., Murakami, T., Stephenson,
636 J. R., Daniel, S., Fukata, M., Hall, R. A., Olson, J. J., Neigh, G. N., Smith, Y., Rainnie, D. G., Van
637 Meir, E. G., 2015. BAI1 regulates spatial learning and synaptic plasticity in the hippocampus. *J*
638 *Clin Invest.* 125, 1497-508.<https://10.1172/JCI74603>.

639 Zhu, D., Osuka, S., Zhang, Z., Reichert, Z. R., Yang, L., Kanemura, Y., Jiang, Y., You, S., Zhang, H., Devi, N.
640 S., Bhattacharya, D., Takano, S., Gillespie, G. Y., Macdonald, T., Tan, C., Nishikawa, R., Nelson, W.
641 G., Olson, J. J., Van Meir, E. G., 2018. BAI1 Suppresses Medulloblastoma Formation by Protecting
642 p53 from Mdm2-Mediated Degradation. *Cancer Cell*. 33, 1004-1016
643 e5.<https://10.1016/j.ccell.2018.05.006>.

644 Zhu, X. B., Wang, Y. B., Chen, O., Zhang, D. Q., Zhang, Z. H., Cao, A. H., Huang, S. Y., Sun, R. P., 2012.
645 Characterization of the expression of macrophage inflammatory protein-1alpha (MIP-1alpha)
646 and C-C chemokine receptor 5 (CCR5) after kainic acid-induced status epilepticus (SE) in juvenile
647 rats. *Neuropathol Appl Neurobiol*. 38, 602-16.<https://10.1111/j.1365-2990.2012.01251.x>.

648

649